ARTICLE OPEN

Recruitment of CCR5^{+} inflammatory monocytes in pulmonary tissue contributes to acute lung injury

Dongdong Wei[1,2,4], Xuebiao Li[1,2,4], Guocong Xu[1,2], Yupeng Sun[1,2], Xian Zhu[1,2], Qunjun Duan[1,2], Ning Gao[3], Aiqiang Dong[1,2] and Minjian Kong[1,2]✉

© The Author(s) 2025

Acute lung injury (ALI) is a common serious complication following deep hypothermic circulatory arrest (DHCA). Monocytes and macrophages play crucial roles in producing inflammatory mediators and regulating innate and adaptive immunity. In our specific rat model of DHCA-induced ALI, we previously showed that autophagy actually has a detrimental effect on lung injury rather than a protective effect. Recently, we reported that monocytes serve an important role in this model. Here, single-cell RNA sequencing was performed on lung tissue cells collected from healthy rats and rats after DHCA. Notably, there was a selective and dramatic increase in the subpopulation of CD43^{low} monocytes in the DHCA group, which expressed high levels of CCR5 and exhibited a proinflammatory phenotype. Allosteric CCR5 drug blockade not only reduced CCR5 expression and alleviated lung injury but also, interestingly, inhibited autophagy. These results suggest that the recruitment of CCR5^{+} inflammatory monocytes into pulmonary tissue contributes to ALI after DHCA and that blocking CCR5 is a plausible intervention for DHCA-induced lung injury by modulating autophagy.

Genes & Immunity (2026) 27:106–116; https://doi.org/10.1038/s41435-025-00371-1

INTRODUCTION

Deep hypothermic circulatory arrest (DHCA) is a special type of cardiopulmonary bypass (CPB), which is currently a necessary technique for cardiac surgery, such as complex congenital heart disease and aortic arch surgeries. This technique reduces hypoxic injury during surgery and decreases postoperative complications but may also cause some potential complications, including acute lung injury (ALI) [1]. Approximately two-thirds of patients develop varying degrees of pulmonary dysfunction postoperatively, with approximately 20% of these patients requiring prolonged mechanical ventilation. The most severe form of lung injury is acute respiratory distress syndrome (ARDS), which has a mortality rate of 80% [2, 3]. The pathophysiologic process of lung injury involves damage to the pulmonary epithelium and vascular endothelium, leading to destruction of the intra- and extracellular matrix, which in turn triggers an inflammatory response [4]. The main mechanisms by which CPB can have deleterious effects on the lungs include blood–circuit interactions, pulmonary ischaemia–reperfusion injury, respiratory arrest, endotoxin, hypothermia, and heparinisation/proteolysis [5, 6]. These mechanisms can induce local or systemic inflammatory response syndrome (SIRS) through a variety of pathways [4, 7].

Monocytes, macrophages, and polymorphonuclear neutrophils (PMNs) are central components of the innate immune system and play important roles in regulating the inflammatory response [8–10]. The activation and polarization of monocytes/macrophages are initiated by pattern recognition receptors (PRRs) that recognize two types of molecular motifs: pathogen-associated molecular patterns (PAMPs), which are evolutionarily conserved structures associated with pathogens such as viruses, bacteria, fungi, and parasites, and damage-associated molecular patterns (DAMPs), which are endogenous molecules that are released in response to tissue damage [11]. Under pathological conditions, monocytes are the main source of effector cells, which are recruited to sites of inflammation and differentiate into inflammatory macrophages and dendritic cells in tissues [12]. The phenotype of activated monocytes/macrophages in different diseases may differ considerably depending on differences in invading pathogens and the type of infection [13]. mRNA sequencing performed by Lan N. Tu's team on total circulating cells from patients after CPB identified myeloid cells, specifically monocytes, as the main cell type driving transcriptional processes after CPB [14]. C-C chemokine receptor 5 (CCR5), a heptameric transmembrane protein similar to the G protein-coupled receptor, is expressed mainly in subpopulations of monocytes, macrophages, dendritic cells, and T lymphocytes [15]. Ligands for CCR5 include monocyte chemotactic protein-2 (MCP-2), macrophage inflammatory protein-1α (MIP-1α/C-C motif chemokine ligand 3, CCL 3), and macrophage inflammatory protein-1β (MIP-1β/CCL4) and are regulated upon activation, normal T-cell expression and secretion (RANTES/CCL5) [16]. Daniel R. Calabrese's team at the University of California reported that CCR5-expressing NK cells were increased in the lungs and airways of bronchoalveolar lavage fluid samples from patients with lung injury after lung

[1]Department of Cardiovascular Surgery, The Second Affiliated Hospital of Zhejiang University School of Medicine, Hangzhou, China. [2]State Key Laboratory Transvascular Implantation Devices, Hangzhou, China. [3]Department of Thoracic Surgery, The First Affiliated Hospital of Sun Yat-sen University, Guangzhou, China. [4]These authors contributed equally: Dongdong Wei, Xuebiao Li. ✉email: kmj@zju.edu.cn

Received: 3 March 2025 Revised: 10 November 2025 Accepted: 24 November 2025
Published online: 24 December 2025

transplantation [17]. Increased CCR5 ligands are associated with increased morbidity in patients, and the use of a pharmacological blocker of CCR5 attenuated I/R-induced lung injury in animal studies [17]. Previous articles have reported that the expression of CCR5, as well as its ligands, on monocytes is elevated in blood samples from patients with alveolar hypoplasia [18]. CCR5 enhances monocyte movement and increases monocyte/macrophage infiltration in the lungs as well as IL-1β levels [18]. These authors concluded that increased CCR5 expression is a key mechanism and potential therapeutic target for the development of this disease and that strategies that target immune cell subsets that express CCR5 deserve further exploration. While monocytes play a critical role in the complex pathophysiology of DHCA-induced lung injury, the specific contribution of CCR5-overexpressing monocyte subpopulations remains unexamined.

Autophagy is an intracellular self-regulatory mechanism that helps maintain homoeostasis within cells by encapsulating waste products, damaged organelles, and excess proteins into vesicles and degrading them [19–21]. Although autophagy typically plays an important role in cell protection, when the autophagy process is abnormal or excessive, it may lead to cell death.

To date, few studies have focused on the role of the regulation of monocyte subpopulations with high expression of CCR5 in DHCA-mediated lung injury, and whether there are changes in autophagic activity among these subpopulations is unknown. Therefore, the aims of this study were (1) to investigate changes in the number of highly expressed CCR5 monocytes in lung tissue samples from rats after DHCA; (2) to determine whether changes in the number of $CCR5^+$ monocytes play a critical role in DHCA-induced lung injury; and (3) to assess whether the use of CCR5 inhibitors affects DHCA-mediated lung injury via alterations in autophagic activity.

METHODS

We declare that all the data that support the findings of this study are available within the article and its Supplemental Materials.

Whole blots on PVDF membranes are available in the Supplemental Materials.

Rats

Male Sprague–Dawley (SD) rats aged approximately 12 weeks and weighing approximately 400 g were housed in a pathogen-free barrier facility for all experiments. Animals were purchased from the Slacas Animal Centre (Shanghai, China). The animal experiments were performed according to the Guide for the Care of Use of Laboratory Animals published by the National Institutes of Health (NIH Pub. No. 85-23, revised 1996), and the research protocol was approved by the Institutional Animal Care and Use Committee of Zhejiang University School of Medicine.

Experimental models of DHCA

DHCA model techniques were performed according to our previously published methods [22, 23]. In brief, the rats were rewarmed after hypothermia and circulatory arrest process, rewarming to a subscalp temperature of 36 °C was recorded at 0 h after DHCA, and the rats were euthanized for sampling at 6 h postoperatively.

Protocol I. To assess the change of monocytes in lung tissue, ten SD rats were randomly assigned and divided into two groups ($n = 5$). In the sham group (Sham group), all rats underwent the same steps without standard DHCA procedures. The DHCA 6 h group (DHCA group) rats experienced standard DHCA intervention and were sacrificed at 6 h after DHCA. Flow cytometry analysis and immunofluorescence was assessed for each group of rats.

Protocol II. To describe the role of monocytes in lung injury induced by the DHCA procedure, clodronate-liposomes (Clo-Lip, 50 mg/kg, i.v. C-010, Liposoma BV, The Netherlands) or control-liposome (PBS) was administered 24 h prior to DHCA. Flow cytometry analysis and immunofluorescence was assessed for each group of rats. And the extent of lung injury, including lung histology examination, wet/dry lung weight ratio, and inflammatory cytokine quantification, was assessed for each group of rats.

Protocol III. To assess whether suppression (maraviroc, MVC, UK-427857, MedChemExpress, China, jugular vein injection) of CCR5 can modulate the lung injury induced by DHCA. MVC or its corresponding solvents (10% DMSO + 40% PEG300 + 5% Tween-80 + 45% saline) was injected half an hour prior to DHCA. Flow cytometry analysis, immunofluorescence, and Western blotting was assessed for each group of rats. Lung injury severity was also assessed.

Animal euthanasia and tissue handling

After the rats were anaesthetized via injection of an overdose of sodium pentobarbital (100 mg/kg, i.p.), lung tissue samples were taken after blood sampling from the abdominal aorta. The rats had a total of five lung lobes: the left lung, the anterior lobe of the right lung, the middle lobe of the right lung, the posterior lobe of the right lung, and the accessory lobe of the right lung.

The experimental protocols and uses of the various parts of the lung tissue were as follows. (1) The anterior lobe of the right lung was first ligated, after which the lung tissue was cut at the distal end of the ligature line and fixed in 10% neutral formalin solution (AG2160, ACMEC Biochemical, Shanghai, China). It was used for subsequent preparation of paraffin sections. (2) The middle lobe of the right lung was ligated, and it was weighed (wet weight) after drying its surface moisture for wet/dry weight ratio analysis. The left auricle was clipped, 100 ml of 4 °C saline was instilled from the right ventricle into the pulmonary circulation until the lung tissue became porcelain white, and all remaining lung lobes were harvested. (3) The posterior lobe of the right lung was used to retain bronchoalveolar lavage fluid (BALF). (4) A portion of the left lung tissue was prepared for single-cell suspensions, and the remaining portion of the left lung was immediately stored in liquid nitrogen for Western blotting.

Flow cytometry analysis

Approximately 100 mg of lung tissue was rinsed in a Petri dish containing PBS at pH 7.2 to remove the remaining blood. The lung tissue was transferred into a gentleMACS tube containing approximately 2.5 mL of enzyme mixture (No. 130-095-927; Miltenyi Biotec, Germany), and the sample was subsequently processed via a gentleMACSTM Dissociator (No. 130-093-235; Miltenyi Biotec, Germany). The cell clumps were removed via filtration with a 300-mesh nylon membrane. After centrifugation (2000 rpm, 5 min, 4 °C), the precipitate was mixed with 500 μL of saline by shaking, resulting in a single-cell suspension of lung tissue to be tested. The antibodies used were as follows: CD45 (2202226, Biolegend, America), CD43 (202812, Biolegend, America), CD172α (sc-376884, Santa Cruz, America), and CCR5 (FAB1802A, R&D Systems, America).

Histological assessment of lung injury

The anterior lobe of the right lung was fixed in formalin for 12–72 h and then dehydrated before paraffin embedding. Sections (3 mm thick) were cut and subjected to haematoxylin and eosin (H&E) staining. After staining, the sections were scanned and analysed with 120 P digital section scanning equipment (Tao Han Medical Technology, Shanghai). Histopathological analyses were performed by three uninformed researchers in a blinded fashion and were scored in detail as described previously [24].

Quantification of cytokines in the lung tissue and BALF

After the rats were euthanized, an appropriate amount of left lung tissue was prepared into tissue homogenate and preserved for further analysis. The posterior lobe of the right lung was rinsed with ice-cold saline and then placed in a disposable Petri dish. Two ml of ice-cold saline was perfused into the alveoli, and the lung tissue was gently massaged to obtain lavage fluid. This step was repeated 20 times, and the fluid collected in the Petri dish was BALF (approximately 1.6 ml). The supernatant was retained after centrifugation (400 × *g*, 5 min at 4 °C) and stored at −80 °C for further analysis. A bicinchoninic acid (BCA) protein assay kit (23227, Thermo Fisher Scientific, Shanghai) was used to determine the total protein concentration in the BALF supernatant.

The protein levels of interleukin-1β (IL-1β), interleukin-6 (IL-6), and tumour necrosis factor α (TNF-α) in the lung tissue and BALF supernatants were measured via ELISA kits (Elkbiotech, Wuhan, China).

Lung wet/dry weight ratio

The middle lobe of the right lung was obtained, rolled over absorbent paper 3 times to dry the surface moisture, weighed, and recorded as wet

weight (W). Afterwards, it was dried in an oven (at 58 °C) until a stable dry weight (D) was reached. The ratio of wet weight to dry weight (W/D) was calculated to assess the degree of pulmonary oedema.

Western blot

The left lung was stored in liquid nitrogen for protein quantification via Western blotting. The tissues were homogenized and lysed in RIPA lysis buffer. The protein concentration was measured via a BCA assay (23225, Thermo Fisher, Shanghai). Protein samples were subjected to gel electrophoresis via SDS–PAGE and then transferred to a polyvinylidene fluoride membrane. Nonspecific binding was blocked with either 5% (w/v) nonfat milk in PBS containing 0.1% (v/v) Tween-20 for 1 h at room temperature, after which the membranes were incubated with the indicated primary antibodies overnight at 4 °C, followed by incubation with secondary antibodies conjugated with horseradish peroxidase. Detection was performed using SuperSignal Substrates (Thermo Fisher, 34577 or 34095). The primary antibodies used were as follows: anti-LC3-I/II (4108, Cell Signalling Technology, Shanghai), anti-ATG5 (10181-2-AP, Proteintech, America), anti-Beclin 1 (11306-1-AP, Proteintech, America), anti-SQSTM1/p62 (ab91526, Abcam, Shanghai), and anti-CCR5 (PA5-114965, Thermo Fisher, Shanghai). Western blotting was assessed for *Protocol III*.

Rat lung single-cell RNA sequencing (scRNA-seq)

Fresh lung tissues were taken from the Sham and DHCA groups for scRNA-seq. In brief, the prepared single-cell suspensions were loaded onto a Chromium Single Cell Controller instrument (10 × Genomics, Pleasanton, CA, USA) to create single-cell gel beads in emulsions for subsequent sequencing and analysis. Single-cell RNA-seq libraries were prepared using a Chromium Single-cell 3′ Reagent Kit, version 2, according to the manufacturer's protocol. The cells were visualized using a 2-dimensional t-SNE algorithm with the RunTSNE function. GO enrichment and KEGG pathway enrichment analyses of the DEGs were performed using R based on the hypergeometric distribution.

Immunofluorescence staining

First, the paraffin sections were deparaffinised and hydrated, and hydrogen peroxide was added to block endogenous peroxidase activity. Second, the sections were boiled in boiling antigen repair solution (1 mmol Tris-EDTA pH = 9.0) for 15 min and incubated in 5% BSA (B2064, Sigma) blocking solution for 20 min at room temperature. Next, the primary antibody CCR5 (PA5-114965, Thermo Fisher, 1:400, 100 µl, overnight at 4 °C) and the corresponding secondary antibody (red, 30 min at 37 °C) were added sequentially, followed by incubation with Try-488 tyramine converting reagent (Bry-Try488, Runnerbio, 20 min at room temperature). After washing, the following steps were repeated: antigen repair, blocking, incubation with CD172α (sc-376884, Santa Cruz, America), incubation with the corresponding secondary antibody (green), and incubation with Try-Cy3 tyramine conversion reagent (Bry-Try-Cy3, Runnerbio, Shanghai). Finally, the sections were washed and incubated with anti-fade mounting medium containing DAPI (P0131, Beyotime, Shanghai) for 30 min. Images were acquired under a fluorescence microscope (Nikon Eclipse Ci-L, Nikon, Japan).

Statistical analysis

With the exception of the scRNA-seq data, *t* tests were employed for normally distributed continuous variables between two groups, and one-way ANOVA followed by Tukey's honest significant difference (HSD) post hoc test was used for comparisons between at least three independent groups. The nonparametric Mann–Whitney U test was used for the lung injury score. The experimental data were analysed using GraphPad Prism software (version 8.0.1; GraphPad Software, Inc., San Diego, CA). The normal distribution of the samples was tested via the Shapiro–Wilk test. Differences were considered statistically significant when the p value was < 0.05.

RESULTS

Monocyte recruitment in lung tissue was increased following DHCA

Our previous results revealed that the expression of the proinflammatory cytokines IL-6 and TNF-α was elevated in the lung tissue and BALF at 6 h after DHCA [22]. These two cytokines are mainly secreted by monocytes/macrophages [25]. Thus, we decided to test whether there was a change in the monocyte proportion (see Protocol I for details). As shown in Fig. 1A, B, flow cytometry analysis revealed that the proportion of monocytes was significantly greater in the DHCA group than in the Sham group. In line with these findings, the immunofluorescence results revealed an increased proportion of monocytes (Fig. 1C, D). These results suggest that monocyte recruitment occurs in lung tissue.

Removal of monocytes alleviated pulmonary injury

To further clarify the role of monocytes in postoperative lung injury after DHCA, Clo-Lip (50 mg/kg) was given intravenously 24 h before DHCA in rats to eliminate monocytes in vivo. Similarly, control-liposomes (PBS, 50 mg/kg) were injected as controls (see Protocol II for details).

Flow cytometry revealed a significant decrease in the proportion of monocytes in the lung tissue of the Clo-Lip group (Fig. 2A, B), which was further confirmed by immunofluorescence (Fig. 2C, D). HE staining revealed that intravenous administration of Clo-Lip 24 h before surgery improved the pathological changes in the lungs after DHCA. The specific manifestations included marked relief of pulmonary interstitial capillary dilation and congestion, alveolar haemorrhage, interstitial oedema and microvascular barrier damage (Fig. 2E, F). Decreased lung tissue injury secondary to DHCA was further confirmed by decreases in BALF protein levels (Fig. 2G), wet/dry weight ratios (Fig. 2H) and levels of inflammatory cytokines (Fig. 2I). Taken together, these results suggest that DHCA-induced lung injury was significantly attenuated after the removal of monocytes with Clo-Lip.

A selective increase in CCR5^{+} inflammatory monocytes

Under pathological conditions, the subpopulation of leucocytes that are mobilized and activated depends largely on the type and site of injury. To better understand the local microenvironment of lung tissues after DHCA in rats, we analysed the lung tissue cells of healthy rats and rats after DHCA for the first time via scRNA-seq. We identified a total of 13 identities via analysis, including monocytes, macrophages, and PMNs. Subpopulations of monocytes in rat lung tissues after DHCA showed significant changes, and monocytes were classified into 4 clusters according to the expression of CD43 (encoded by the Spn gene, Fig. 3A): mature CD43^{high} monocytes (clusters 1, 3) and naïve CD43^{low} monocytes (clusters 2, 4). The results revealed that the Sham group was dominated by clusters 1 and 4, which were mainly mature cells with high CD43 expression (up to 68.4%). The DHCA group was dominated by clusters 2 and 3, which were mainly naïve cells with low CD43 expression (up to 66.6%), suggesting the selective recruitment of monocyte subpopulations. Significant changes in immune cells were observed in the lung tissues of the rats after DHCA. Notably, there was a selective and dramatic increase in the subpopulation of CD43^{low} naïve monocytes among the monocytes of the DHCA group. Cluster 2 of CD43^{low} monocytes in the DHCA group highly expressed CCR5, S100A8, S100A9, Nos2, Vegfa, IL-1β, etc., and exhibited proinflammatory polarization (Fig. 3B, C, the clearer differential expression plots see Fig. S1). Gene Ontology (GO) enrichment analysis showed top 30 GO term was associated with monocyte chemotaxis and inflammatory response (Fig. 3D, E). By integrating scRNA-seq data from defined cellular subpopulations with the ligand-receptor interaction database (CellPhoneDB), we systematically mapped ligand and receptor expression profiles across cell types (new Fig. 3F). Genes closely related to leucocyte migration, macrophage activation and other inflammation-related signalling pathways were significantly upregulated in monocytes from the DHCA group compared with those from the control group (Fig. 3G).

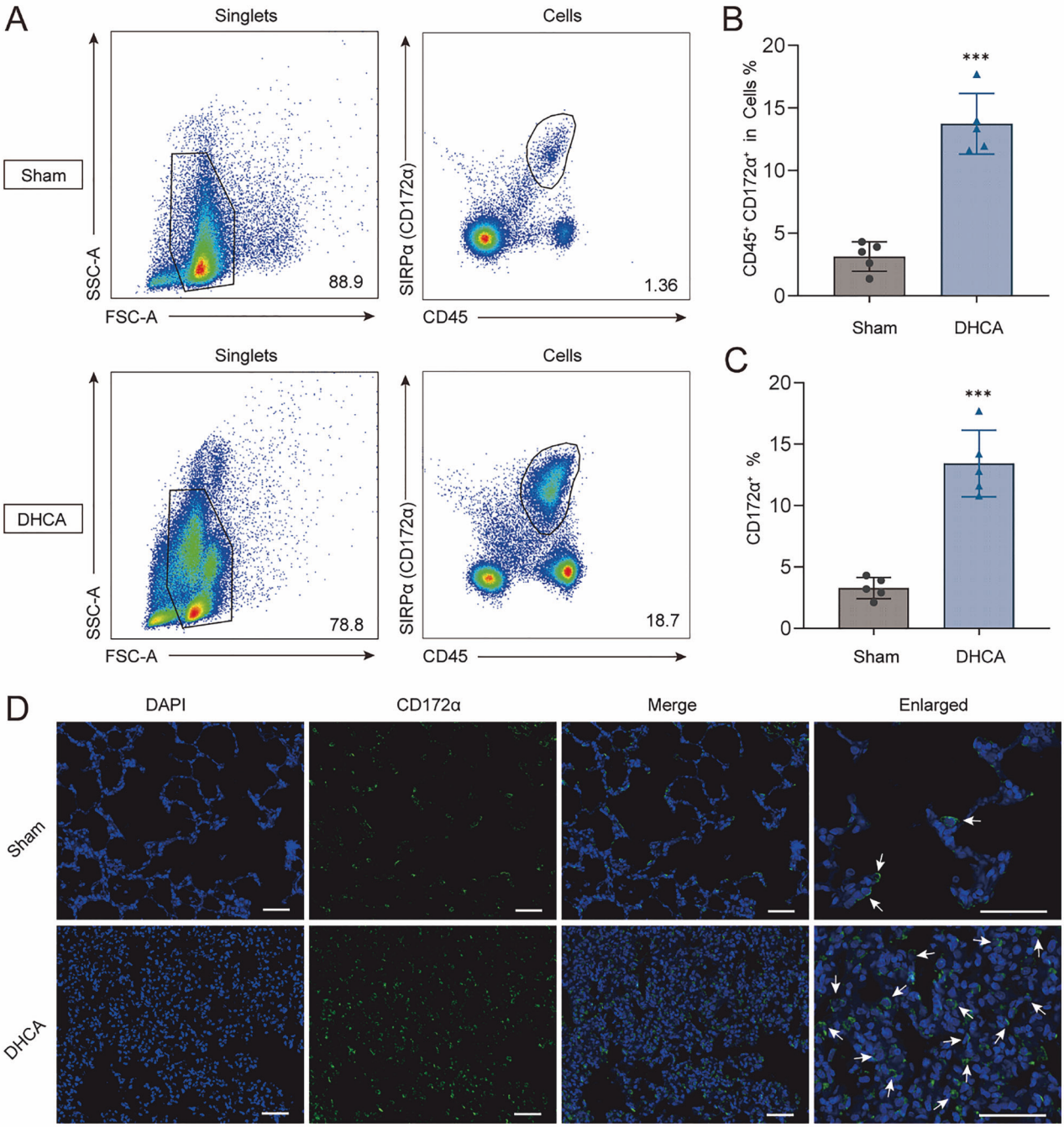

Fig. 1 Increased proportion of monocytes in lung tissue in the DHCA group. A Representative flow cytometry of monocytes in rat lung tissue showed an increased proportion of monocytes in the DHCA group. SIRPα (CD172α) is a specific marker for rat monocytes. Numbers in the flow plot correspond to the percentage of the parent population. **B** Bar graph showed the proportion of monocytes among cells in rat lung tissue ($n = 5$). **C**, **D** Compared to the Sham group, immunofluorescence staining for CD172α showed a significant increase in the number of puncta in the DHCA 6 h group (Scale bar = 50 μm). Green, CD172α-positive cells; blue, DAPI-stained nuclei. Quantitative analysis is shown in (**C**; $n = 5$). *, $p < 0.05$; **, $p < 0.01$; ***, $p < 0.001$.

CCR5 blockade reduced lung injury and inhibited autophagy

The selective dramatic increase in the $CD43^{low}CCR5^{+}$ monocyte subpopulation after DHCA, as well as attenuation of DHCA-induced lung injury after monocyte removal with Clo-Lip, was observed. To further validate the role of this population of cells, we administered maraviroc (MVC, the CCR5-specific inhibitor) half an hour prior to DHCA procedure (see Protocol III for details). Flow cytometry analyses revealed that MVC significantly reduced the proportion of $CCR5^{+}$ monocytes (Fig. 4A–C), which was further confirmed by immunofluorescence (Fig. 4D, E) and Western blotting (Fig. 4F, G; full blots are shown in Fig. S2B). Moreover, we found that compared with DHCA, MVC attenuated lung injury, as evidenced by alleviated alveolar septal congestion, pulmonary oedema and inflammatory cell infiltration, as shown by histological examination (Fig. 5A, B). Furthermore, quantification of both the protein content in the BALF (Fig. 5C) and the wet/dry weight ratio (Fig. 5D) yielded similar results. The improvement in lung injury was associated with a trend towards reductions in the levels

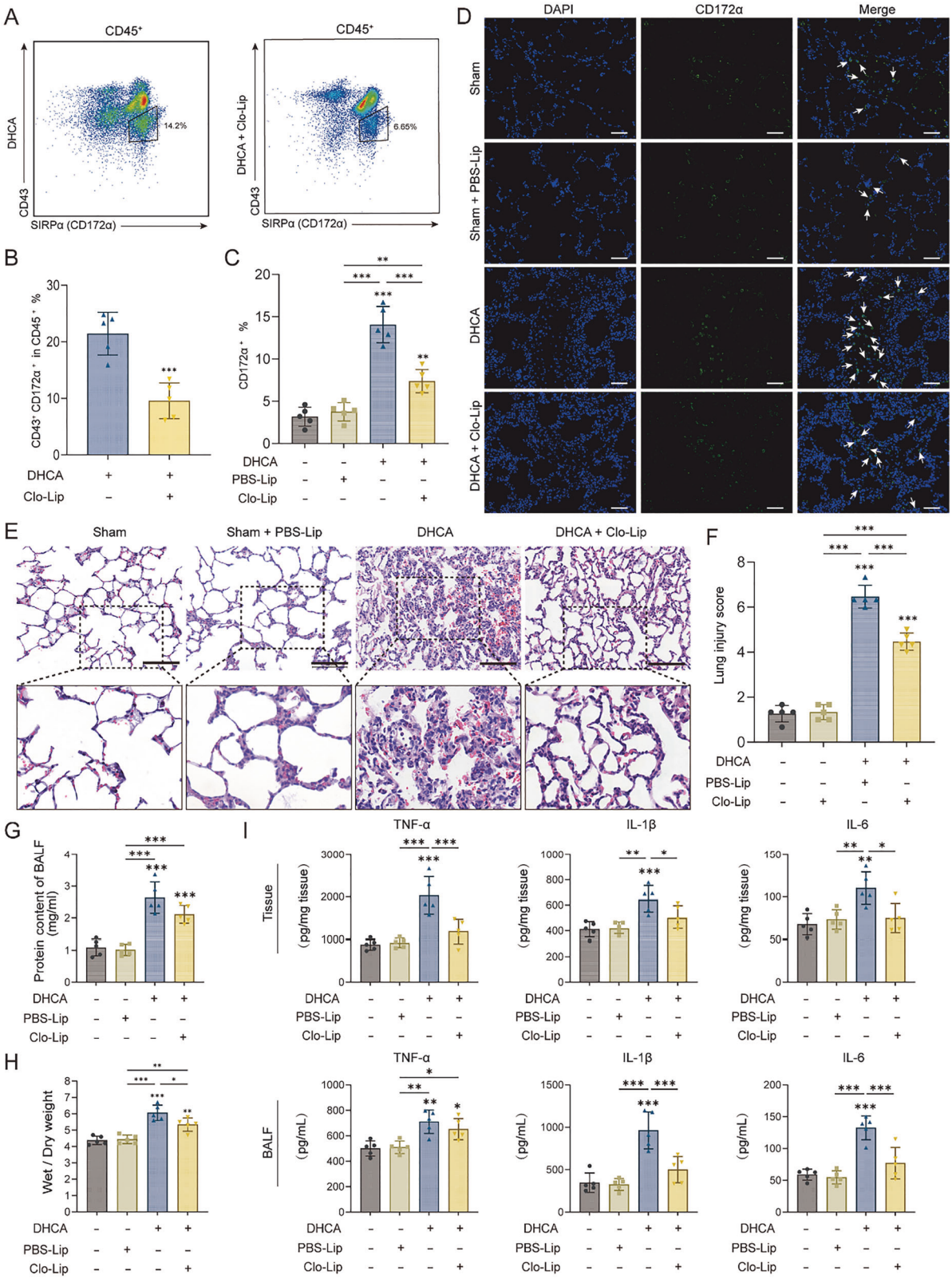

of inflammatory factors in the lung tissue (Fig. 5E). Autophagy machinery proteins, including LC3-II, Beclin 1, ATG5, and p62, were measured in different groups to assess autophagy activity. Compared with those in the Sham group, the expression levels of LC3-II, Beclin 1, and ATG5 clearly increased in the DHCA group, indicating that autophagy was activated after DHCA. In contrast, after the administration of MVC, the autophagy-related protein expression in the rats recovered (Fig. 5F, G; whole blots are shown in Fig. S2B), which eventually approached the level of autophagy in the Sham group. Interestingly, the role of Clo-Lip was similar to

Fig. 2 DHCA-induced lung injury was attenuated after clodronate was given intravenously 24 h before surgery. Twenty SD rats were randomly divided into 4 groups: Sham group, DHCA group, Clo-Lip group and PBS-Lip serving as the placebo for a control group. Rats in the Clo-Lip group experienced standar DHCA intervention 24 h after i.v. injection of Clo-Lip ($n = 5$ independent experiments). **A** Flow cytometry of monocytes in lung tissue from rats undergoing the DHCA procedure showed a decreased proportion of monocytes 24 h after PBS or Clo-Lip injection ($n = 5$ rats per group). **B** Bar graph showing the proportion of monocytes among leucocytes and that preoperative administration of Clo-Lip significantly reduced the proportion of monocytes in lung tissue 6 h after DHCA. **C**, **D** Compared to the DHCA group, immunofluorescence staining for CD172α showed a significant decrease in the number of puncta in the Clo-Lip group (Scale bar = 50 μm). Green, CD172α-positive cells; blue, DAPI-stained nuclei. Quantitative analysis is shown in (**C**; $n = 5$). **E** Representative haematoxylin and eosin staining images in DHCA 6 h group and Clo-Lip group. The DHCA group rats exhibited prominent alveolar inflammatory cells infiltration, interstitial capillary vessel dilatation and congestion, alveolar haemorrhage and interstitial oedema. The use of Clo-Lip significantly mitigates these histopathologic impairments (Scale bar = 100 μm). **F** Histologic analysis for lung injury. The total histopathological score was expressed as the sum of the scores for all parameters. **G** Total alveolar protein concentration was significantly reduced in the Clo-Lip group compared to the DHCA group. **H** Lung wet/dry weight ratio also decreased in the Clo-Lip group. **I** The levels of inflammatory factors in bronchoalveolar lavage fluid (BALF) and lung tissue were significantly decreased when Clo-Lip group compared to the DHCA group. *, $p < 0.05$; **, $p < 0.01$; ***, $p < 0.001$.

that of MVC in this model (Fig. S3A–D; full blots are shown in Fig. S2A). Taken together, these data suggest that the use of CCR5-specific inhibitors reduces CCR5 expression in monocytes and could have a therapeutic effect on DHCA-induced lung injury.

DISCUSSION

Our group has successfully established a mature and stable rat DHCA model. Based on these findings, we revealed in our previous study that lung injury in rats dynamically changed within 24 h after DHCA: lung injury was relatively mild from 1 to 3 h, and lung tissue damage was the most severe at 6 h after surgery and partially recovered at 24 h after the operation [22]. This result preliminarily revealed that lung injury occurred mainly approximately 3–6 h after DHCA; thus, 6 h after DHCA was chosen as the optimal time point for an in-depth exploration of the mechanisms of DHCA-mediated ALI.

We observed that, at 6 h after DHCA, in addition to severe lung injury, there was increased recruitment of monocytes to the lung tissue in the DHCA group compared with the Sham group. To validate the role of monocytes in lung injury, we used the currently preferred method of transient mononuclear phagocyte (MoPh) depletion in many laboratories worldwide, i.e., intravenous Clo-Lip administration before surgery. We found that the extent of lung damage was significantly reduced after the elimination of monocytes. Therefore, we analysed the lung tissue cells of healthy rats and rats after DHCA for the first time via scRNA-seq. A subset of $CD43^{low}$ monocytes that highly expresses CCR5 was described in rats after the DHCA procedure. Moreover, CCR5 blockade reduced lung injury, and interestingly, autophagy levels were lower in the CCR5 blockade group than in the experimental group. In our previous study, the most severe moments of lung injury and the highest autophagy levels were observed at 6 h within 24 h after DHCA, and enhanced autophagy was shown to be responsible for DHCA-induced pathological damage, which is consistent with the findings of this study. Therefore, these data suggest that the pathogenicity of infiltrating monocytes could prompt acute inflammation and that the inhibition of CCR5 expression in monocytes is a plausible intervention for DHCA-induced lung injury.

The results of mRNA sequencing of total circulating cells from patients after CPB identified myeloid cells, specifically monocytes, as the main cell type driving transcriptional processes after CPB [14]. The infiltration of monocytes is one of several pathways that drive proinflammatory programmes [26]. Under pathological conditions, monocytes are recruited to sites of inflammation and differentiate into inflammatory macrophages and dendritic cells in tissues, which constitute the main source of effector cells [27]. These activated proinflammatory monocytes/macrophages provide the front-line defence against invading pathogens, producing mainly IL-1β, IL-6, IL-12, IL-23, TNF-α, NO, and ROS, facilitating complement-mediated phagocytosis, and promoting the Th 1 response. Massive inflammatory cell infiltration and elevated proinflammatory cytokine/chemokine responses lead to excessive accumulation of monocytes, macrophages and PMNs in the lungs [28]. Our previous study demonstrated that the expressions of the cytokines TNF-α, IL-1β, and IL-6 were elevated in lung tissue and BALF in the early postoperative period after DHCA in rats. Among them, there was a transient peak in TNF-α and IL-6 levels at 1 h postsurgery, suggesting that there may be an inflammatory storm in the early stage. Activated alveolar macrophages can release more cytokines and inflammatory mediators. Elevated levels of circulating cytokines and immune-cell hyperactivation contribute to the cytokine storm, leading to an uncontrolled inflammatory process that further aggravates injury [29].

Previous studies have shown that increased production of CCR5 ligands during infection can lead to CCR5 overexpression and $CCR5^{+}$ cell recruitment to the perilesion area, resulting in amplification of the local inflammatory response [30]. In addition, CCR5 expression on monocytes, as well as its ligands, is elevated in blood samples from patients with alveolar hypoplasia. CCR5 enhances monocyte movement and increases monocyte/macrophage infiltration in the lungs as well as IL-1β levels [18]. Importantly, CCR5 receptor–ligand interactions may constitute a common mechanism of acute lung injury, independent of aetiology [17]. Maraviroc is an FDA-approved compound that targets this CCR5 pathway and has been shown to be broadly safe in a variety of patient populations at risk [31]. The application of MVC attenuated lung injury, and coincidentally, autophagy levels decreased without changing the autophagy flux [22]. Notably, previous results have shown that autophagic flux was not interrupted at either the early or late phase following DHCA, as chloroquine delivery caused further increases in the expressions of autophagy machinery proteins [22]. The findings concerning the role of autophagy were consistent across both experiments, suggesting that autophagy is deleterious in this specific model of DHCA-mediated lung injury in rats. This experiment further elucidated the role of monocytes in this model. At the same time, we made other observations that are of interest to us for further exploration.

In conclusion, the rats developed severe lung injury and increased autophagy activity at 6 h after DHCA, which was accompanied by increased recruitment of monocytes to the lung tissue. Importantly, pulmonary injury was significantly alleviated after the removal of monocytes. scRNA-seq revealed a selective and dramatic increase in the subpopulation of $CD43^{low}$ naïve monocytes among monocytes in the DHCA group, which highly expressed CCR5. Notably, the MVC-mediated reduction in CCR5 expression attenuated DHCA-induced lung injury and suppressed autophagy in rats. These results suggest that the recruitment of $CCR5^{+}$ inflammatory monocytes into pulmonary

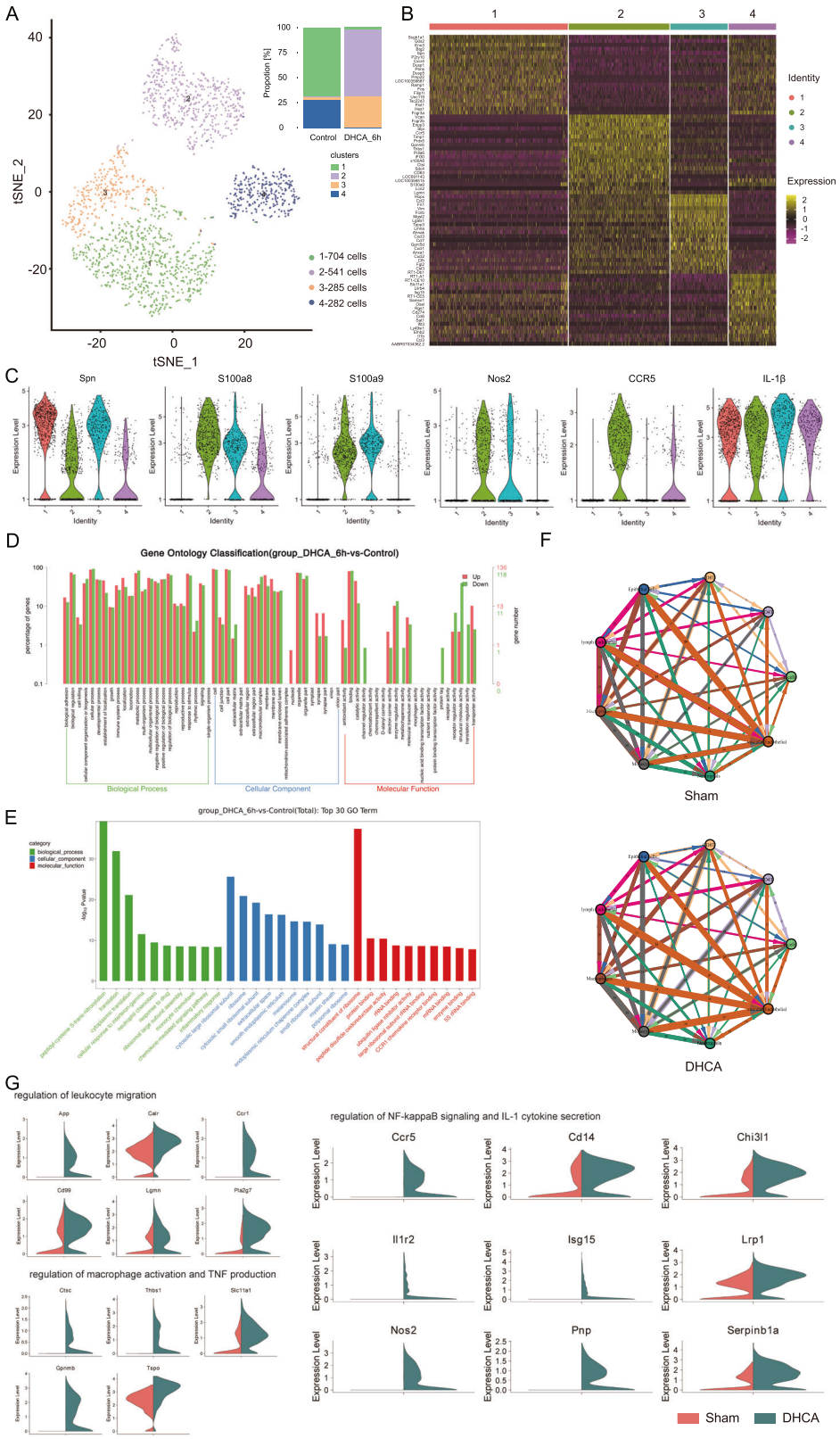

Fig. 3 Heterogeneous changes in monocytes in the lung tissue of the Sham and DHCA groups. A Single-cell RNA sequencing results showing changes in mononuclear subpopulations in lung tissue after DHCA surgery: monocytes were classified into 4 clusters according to CD43 expression: clusters 1 and 4 were predominant in the Sham group; clusters 2 and 3 were predominant in the DHCA group. **B** Heatmap of 4 monocyte subpopulations. **C** Cluster 2 of CD43^{low} monocytes in the DHCA group showed a pro-inflammatory phenotype with high expression of CCR5, S100a8, S100a9, Nos2, Vegfa, and IL-1β. **D**, **E** Gene Ontology (GO) enrichment analysis. **F** Cell communication network. **G** Genes closely related to leucocyte migration, macrophage activation and other inflammation-related signalling pathways were significantly upregulated in monocytes from the DHCA group compared to the control group.

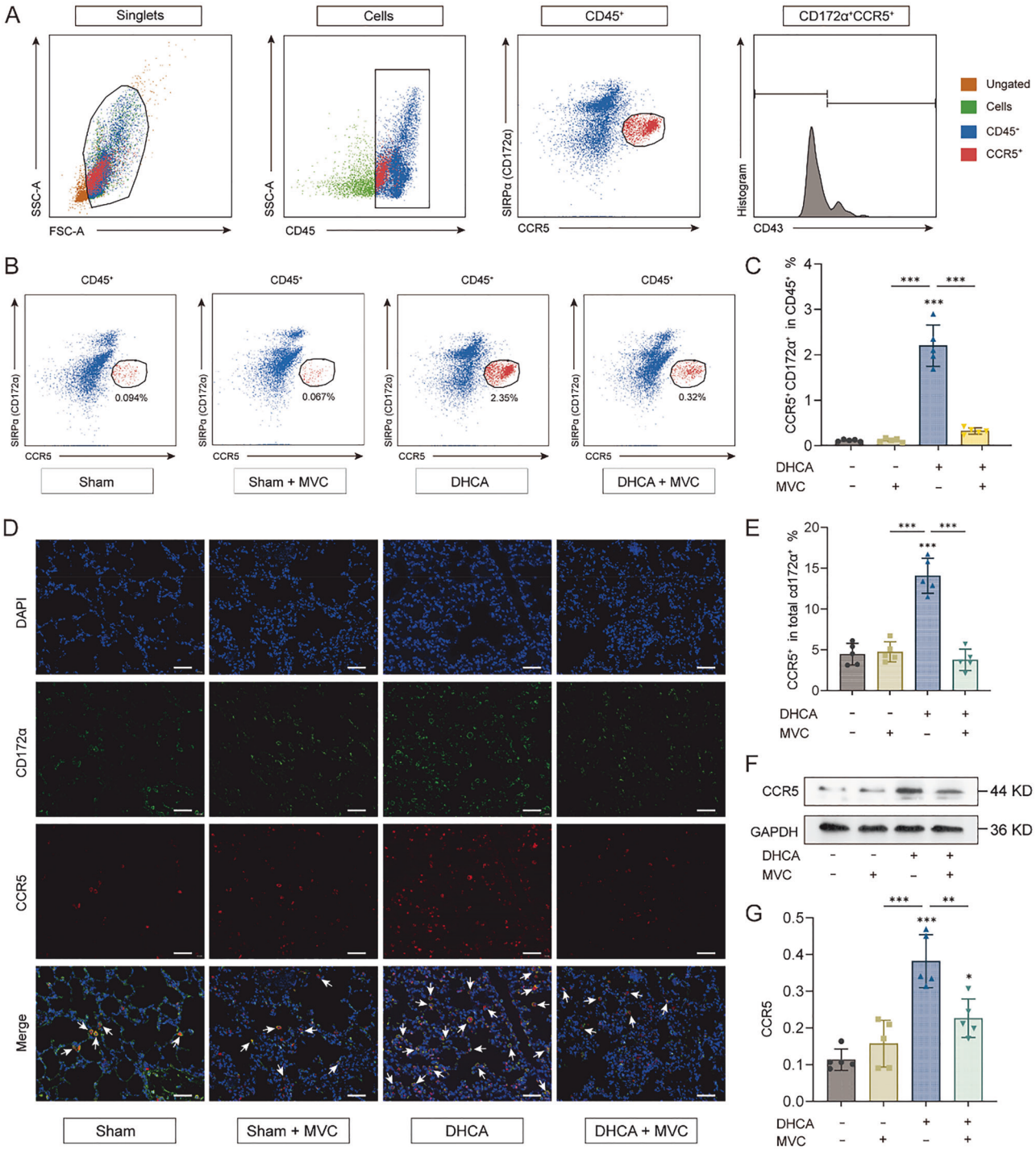

Fig. 4 Intravenous application of MVC half an hour before DHCA significantly reduces CCR5 expression in rat lung tissue. A Gating strategy for $CD45^+CD172\alpha^+CCR5^+$ monocytes. **B** Representative flow cytometry of $CCR5^+$ monocytes showed a decrease in the MVC group compared to the DHCA group. Numbers in the flow plot correspond to the percentage of $CCR5^+$ monocytes in the $CD45^+$ population. **C** Bar graph showed the proportion of $CCR5^+$ monocytes among leucocytes in rat lung tissue ($n = 5$). **D**, **E** Compared to the DHCA group, immunofluorescence staining of CD172α and CCR5 co-staining showed a significant reduction in the number of puncta in the MVC group (Scale bar = 50 μm). Green, CD172α-positive cells; red, CCR5-positive cells; blue, DAPI-stained nuclei. Quantitative analysis is shown in (**E**; $n = 5$). **F**, **G** The expression level of CCR5 was significantly reduced after administration of MVC. Quantitative analysis is shown in (**G**; $n = 5$). *, $p < 0.05$; **, $p < 0.01$; ***, $p < 0.001$.

tissue contributes to lung injury after DHCA and that CCR5 blockade has a therapeutic effect on DHCA-mediated lung injury. However, further studies are needed to elucidate the intrinsic mechanisms by by $CCR5^+$ inflammatory monocytes in our specific rat model of DHCA-induced lung injury.

Study limitations and future perspectives

Clo-Lip has been used by many laboratories worldwide to transiently deplete MoPh to study the function of these cells in vivo. However, Gerhard Krönke's team recently reported that the anti-inflammatory effects of Clo-Lip do not result from the

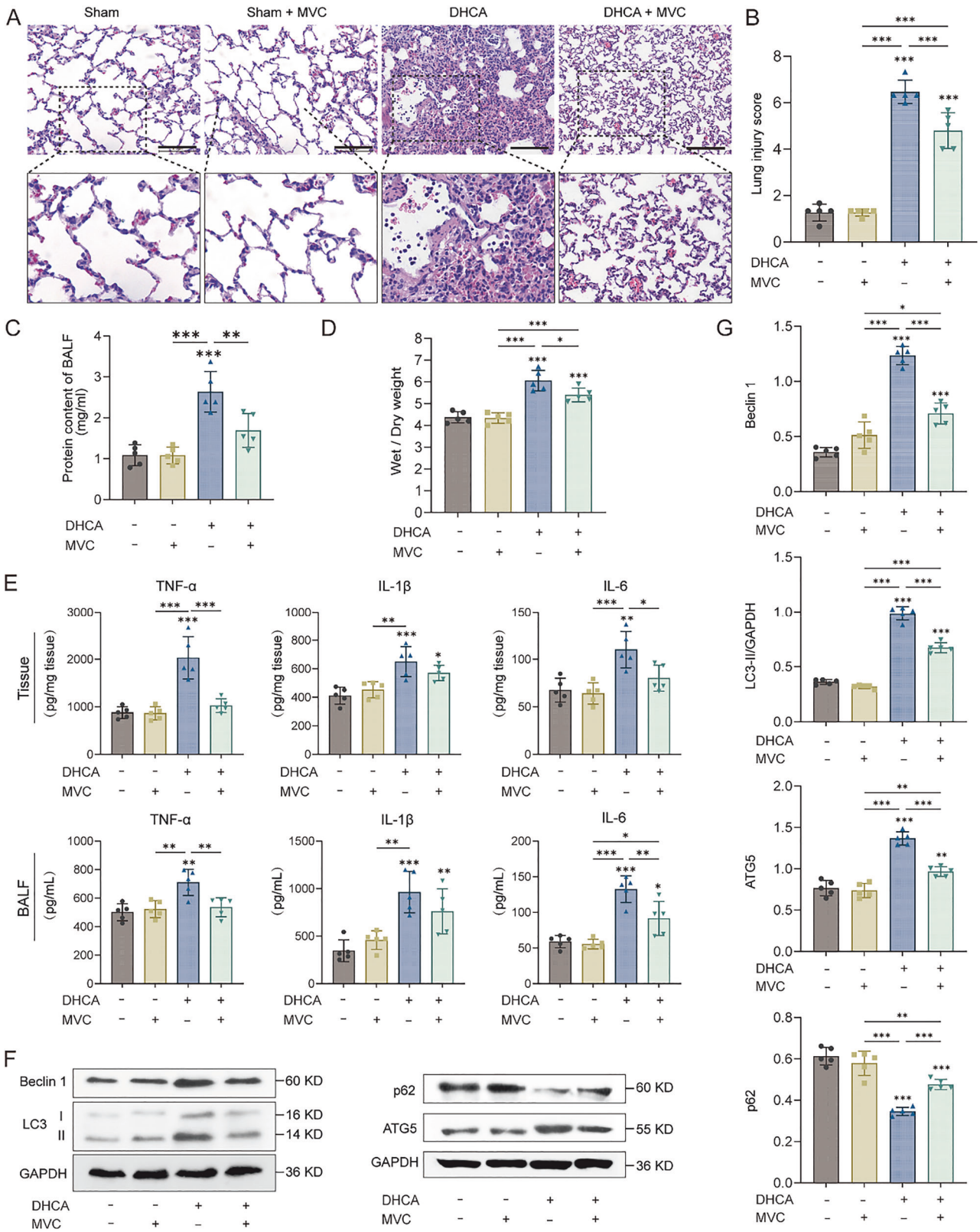

Fig. 5 DHCA-induced lung injury was attenuated by MVC. A Representative haematoxylin and eosin staining images in DHCA 6 h group and MVC group. Compared with the DHCA group, the degree of lung injury in MVC group decreased (Scale bar = 100 μm). **B** Inhibition of CCR5 expression significantly attenuates lung injury score after DHCA. **C** Total alveolar protein concentration was significantly reduced in the MVC group compared to the DHCA group. **D** Lung wet/dry weight ratio also decreased in the MVC group. **E** The levels of inflammatory factors in BALF and lung tissue were significantly decreased when MVC group compared with the DHCA group. *, $p < 0.05$; **, $p < 0.01$; ***, $p < 0.001$. **F**, **G** The expression levels of autophagy-related proteins were significantly reduced after administration of MVC. Quantitative analysis is shown in (**G**; $n = 5$). *, $p < 0.05$; **, $p < 0.01$; ***, $p < 0.001$.

depletion of MoPh but rather from a functional stunning of PMNs [32, 33]. These findings require a re-examination of the current literature regarding the role of monocytes and macrophages in inflammation. Interestingly, our scRNA-seq analysis of rat lung tissues revealed that the most altered cellular composition of lung tissue was neutrophilic and that PMNs in lung tissue were found to be highly expressive of activated, inflammation-associated genes via transcriptomic analysis. The results of Gerhard Krönke's team and the phenomena observed in this study suggest that PMNs may play an important role in this model. Although the role of PMNs was not the focus of this study, the changes in PMNs that we noticed and the effect of Clo-Lip on PMNs attracted our interest, and we would like to explore the role of PMNs and the role of monocyte–neutrophil interactions in the immune microenvironment of lung tissues in the postoperative period after DHCA in depth in subsequent studies.

To our knowledge, intranasal administration of Clo-Lip has been shown to selectively deplete lung-resident alveolar macrophages [34]. However, pre-experimentation with intranasal administration of Clo-Lip in our particular model resulted in more severe lung injury in rats than did intravenous administration (Figure S4). This is likely because intranasal administration decreases dynamic airway compliance and increases airway resistance, leading to increased lung injury [35]. Therefore, we ultimately chose intravenous administration as the mode of delivery. However, the mode of administration warrants further exploration in view of the special characteristics of Clo-Lip.

Moreover, it is important to acknowledge that our measurements of autophagy-related proteins reflect composite signals from multiple cell types within lung tissue. While we observed a concomitant reduction in autophagy markers with attenuated monocyte infiltration after removal of monocytes or inhibition of CCR5, these data cannot definitively attribute changes in autophagic activity to monocytes regulation alone. Future studies employing cell-specific autophagy assays are warranted to clarify this relationship.

In addition, CCR5 may have pleiotropic effects on the lungs in a wide range of target cells. Although we demonstrated a decrease in autophagy during CCR5 blockade, remission of lung injury may also be caused by alternative pathways. Thus, additional work is needed to characterize the dependent and independent effects of autophagy on CCR5 expression in monocytes.

Patents

The patent for the cardiac pulmonary bypass device was published by the State Intellectual Property Office, the application number, 201910261956X.

DATA AVAILABILITY

All data reported herein have been deposited in the Figshare (https://doi.org/10.6084/m9.figshare.29302574). Other queries for data and code could be directly sent to the corresponding author.

REFERENCES

1. Wang Y, Chen L, Yao C, Wang T, Wu J, Shang Y, et al. Early plasma proteomic biomarkers and prediction model of acute respiratory distress syndrome after cardiopulmonary bypass: a prospective nested cohort study. Int J Surg. 2023;109:2561–73.
2. Vlastos D, Zeinah M, Ninkovic-Hall G, Vlachos S, Salem A, Asonitis A, et al. The effects of ischaemic conditioning on lung ischaemia-reperfusion injury. Respir Res. 2022;23:351.
3. Biancari F, Juvonen T, Fiore A, Perrotti A, Hervé A, Touma J, et al. Current outcome after surgery for type A aortic dissection. Ann Surg. 2023;278:e885–e892.
4. Akimova T, Zhang T, Christensen LM, Wang Z, Han R, Negorev D, et al. Obesity-related IL-18 impairs T-regulatory cell function and promotes lung ischemia-reperfusion injury. Am J Respir Crit Care Med. 2021;204:1060–74.
5. Lagier D, Velly LJ, Guinard B, Bruder N, Guidon C, Vidal Melo MF, et al. Perioperative open-lung approach, regional ventilation, and lung injury in cardiac surgery. Anesthesiology. 2020;133:1029–45.
6. Xing Z, Han J, Hao X, Wang J, Jiang C, Hao Y, et al. Immature monocytes contribute to cardiopulmonary bypass-induced acute lung injury by generating inflammatory descendants. Thorax. 2017;72:245–55.
7. Schlapbach LJ, Gibbons KS, Horton SB, Johnson K, Long DA, Buckley DHF, et al. Effect of nitric oxide via cardiopulmonary bypass on ventilator-free days in young children undergoing congenital heart disease surgery: the NITRIC randomized clinical trial. JAMA. 2022;328:38–47.
8. Lazarov T, Juarez-Carreño S, Cox N, Geissmann F. Physiology and diseases of tissue-resident macrophages. Nature. 2023;618:698–707.
9. Ng LG, Liu Z, Kwok I, Ginhoux F. Origin and heterogeneity of tissue myeloid cells: a focus on GMP-derived monocytes and neutrophils. Annu Rev Immunol. 2023;41:375–404.
10. Karimi E, Azari H, Yari M, Tahmasebi A, Hassani Azad M, Mousavi P. Interplay between SARS-CoV-2-derived miRNAs, immune system, vitamin D pathway and respiratory system. J Cell Mol Med. 2021;25:7825–39.
11. Oh S, Lee J, Oh J, Yu G, Ryu H, Kim D, et al. Integrated NLRP3, AIM2, NLRC4, Pyrin inflammasome activation and assembly drive PANoptosis. Cell Mol Immunol. 2023;20:1513–26.
12. Vanneste D, Bai Q, Hasan S, Peng W, Pirottin D, Schyns J, et al. MafB-restricted local monocyte proliferation precedes lung interstitial macrophage differentiation. Nat Immunol. 2023;24:827–40.
13. Bassler K, Schulte-Schrepping J, Warnat-Herresthal S, Aschenbrenner AC, Schultze JL. The myeloid cell compartment-cell by cell. Annu Rev Immunol. 2019;37:269–93.
14. Tu LN, Hsieh L, Kajimoto M, Charette K, Kibiryeva N, Forero A, et al. Shear stress associated with cardiopulmonary bypass induces expression of inflammatory cytokines and necroptosis in monocytes. JCI Insight. 2021;6:e141341.
15. Lin Y, Liu S, Sun Y, Chen C, Yang S, Pei G, et al. CCR5 and inflammatory storm. Ageing Res Rev. 2024;96:102286.
16. Shen Y, Zhou M, Cai D, Filho DA, Fernandes G, Cai Y, et al. CCR5 closes the temporal window for memory linking. Nature. 2022;606:146–52.
17. Santos J, Wang P, Shemesh A, Liu F, Tsao T, Aguilar OA, et al. CCR5 drives NK cell-associated airway damage in pulmonary ischemia-reperfusion injury. JCI Insight. 2023;8:e173716.
18. Chen Z, Xie X, Jiang N, Li J, Shen L, Zhang Y. CCR5 signaling promotes lipopolysaccharide-induced macrophage recruitment and alveolar developmental arrest. Cell Death Dis. 2021;12:184.
19. Dong W, He B, Qian H, Liu Q, Wang D, Li J, et al. RAB26-dependent autophagy protects adherens junctional integrity in acute lung injury. Autophagy. 2018;14:1677–92.
20. Li Y, Liang Z, He H, Huang X, Mo Z, Tan J, et al. The lncRNA HOTAIR regulates autophagy and affects lipopolysaccharide-induced acute lung injury through the miR-17-5p/ATG2/ATG7/ATG16 axis. J Cell Mol Med. 2021;25:8062–73.
21. Klionsky DJ, Abdel-Aziz AK, Abdelfatah S, Abdellatif M, Abdoli A, Abel S, et al. Guidelines for the use and interpretation of assays for monitoring autophagy (4th edition). Autophagy. 2021;17:1–382.
22. Kong M, Wei D, Li X, Zhu X, Hong Z, Ni M, et al. The dynamic changes in autophagy activity and its role in lung injury after deep hypothermic circulatory arrest. J Cell Mol Med. 2022;26:1113–27.
23. Zhu X, Ji B, Liu J, Sun Y, Wu S, Zheng Z, et al. Establishment of a novel rat model without blood priming during normothermic cardiopulmonary bypass. Perfusion. 2014;29:63–9.
24. Wu D, Spencer CB, Ortoga L, Zhang H, Miao C. Histone lactylation-regulated METTL3 promotes ferroptosis via m6A-modification on ACSL4 in sepsis-associated lung injury. Redox Biol. 2024;74:103194.
25. Shi C, Pamer EG. Monocyte recruitment during infection and inflammation. Nat Rev Immunol. 2011;11:762–74.
26. Merad M, Martin JC. Pathological inflammation in patients with COVID-19: a key role for monocytes and macrophages. Nat Rev Immunol. 2020;20:355–62.
27. Qian Y, Wang Z, Lin H, Lei T, Zhou Z, Huang W, et al. TRIM47 is a novel endothelial activation factor that aggravates lipopolysaccharide-induced acute lung injury in mice via K63-linked ubiquitination of TRAF2. Signal Transduct Target Ther. 2022;7:148.
28. Channappanavar R, Perlman S. Pathogenic human coronavirus infections: causes and consequences of cytokine storm and immunopathology. Semin Immunopathol. 2017;39:529–39.
29. Fajgenbaum DC, June CH. Cytokine storm. N Engl J Med. 2020;383:2255–73.
30. Martin-Blondel G, Brassat D, Bauer J, Lassmann H, Liblau RS. CCR5 blockade for neuroinflammatory diseases–beyond control of HIV. Nat Rev Neurol. 2016;12:95–105.
31. Lévy Y, Lelièvre JD, Assoumou L, Aznar E, Pulido F, Tambussi G, et al. Addition of maraviroc versus placebo to standard antiretroviral therapy for initial treatment of advanced HIV infection: a randomized trial. Ann Intern Med. 2020;172:297–305.

32. Mass E. The stunning clodronate. J Exp Med. 2023;220:e20230339.
33. Culemann S, Knab K, Euler M, Wegner A, Garibagaoglu H, Ackermann J, et al. Stunning of neutrophils accounts for the anti-inflammatory effects of clodronate liposomes. J Exp Med. 2023;220:e20220525.
34. Oza D, Ivich F, Pace J, Yu M, Niedre M, Amiji M. Lipid nanoparticle encapsulated large peritoneal macrophages migrate to the lungs via the systemic circulation in a model of clodronate-mediated lung-resident macrophage depletion. Theranostics. 2024;14:2526–43.
35. Nakamura T, Abu-Dahab R, Menger MD, Schäfer U, Vollmar B, Wada H, et al. Depletion of alveolar macrophages by clodronate-liposomes aggravates ischemia-reperfusion injury of the lung. J Heart Lung Transpl. 2005;24:38–45.

ACKNOWLEDGEMENTS

This study was supported by the National Natural Science Foundation of China.

AUTHOR CONTRIBUTIONS

DW and GX wrote the manuscript. DW, GX, XL, YS, XZ, QD, and NG researched data. AD and MK contributed to the discussion and reviewed/edited the manuscript. AD, MK, and DW designed the study, reviewed the data, and revised the manuscript. All authors have read and agreed to the published version of the manuscript.

FUNDING

This research was funded by the National Natural Science Foundation of China (82070275) and Key research and development programme of Zhejiang Province (2025C02143).

COMPETING INTERESTS

The authors declare no competing interests.

ETHICS APPROVAL AND CONSENT TO PARTICIPATE

The animal experiments were performed according to the Guide for the Care of Use of Laboratory Animals published by the National Institutes of Health (NIH Pub. No. 85-23, revised 1996), and the research protocol was approved by the Institutional Animal Care and Use Committee of Zhejiang University School of Medicine.

ADDITIONAL INFORMATION

Supplementary information The online version contains supplementary material available at https://doi.org/10.1038/s41435-025-00371-1.

Correspondence and requests for materials should be addressed to Minjian Kong.

Reprints and permission information is available at http://www.nature.com/reprints

Publisher's note Springer Nature remains neutral with regard to jurisdictional claims in published maps and institutional affiliations.

Open Access This article is licensed under a Creative Commons Attribution-NonCommercial-NoDerivatives 4.0 International License, which permits any non-commercial use, sharing, distribution and reproduction in any medium or format, as long as you give appropriate credit to the original author(s) and the source, provide a link to the Creative Commons licence, and indicate if you modified the licensed material. You do not have permission under this licence to share adapted material derived from this article or parts of it. The images or other third party material in this article are included in the article's Creative Commons licence, unless indicated otherwise in a credit line to the material. If material is not included in the article's Creative Commons licence and your intended use is not permitted by statutory regulation or exceeds the permitted use, you will need to obtain permission directly from the copyright holder. To view a copy of this licence, visit http://creativecommons.org/licenses/by-nc-nd/4.0/.

© The Author(s) 2025